J Mater Sci (2011) 46:7706–7712
DOI 10.1007/s10853-011-5750-y

Growth of hydrophobic TiO_2 on wood surface using a hydrothermal method

Qingfeng Sun · Yun Lu · Yixing Liu

Received: 8 April 2011 / Accepted: 27 June 2011 / Published online: 7 July 2011

Abstract Hydrophobic titanium dioxide (TiO_2) was successfully grown on a wood surface using a hydrothermal method. Energy dispersive X-ray spectroscopy (EDS), Fourier transform infrared spectroscopy (FTIR), X-ray diffraction (XRD), and water contact angle (WCA) were employed to characterize the features of grown TiO_2 and its hydrophobicity. EDS, XRD, and FTIR proved that anatase TiO_2 chemically bonded to the wood surface through the combination of hydrogen groups during the hydrothermal process. The values of WCAs manifested that the hydrophobicity of the treated wood was mainly dependent on specific reaction conditions, especially on reaction pH value and hydrothermal temperature. The highest WCA reached 154° when the hydrothermal temperature was 130 °C. The treated wood thus possessed a superhydrophobic surface.

Introduction

Wood is a natural polymer composite that can be subjected to a wide variety of treatments to make it suitable for specific technical applications. The greatest disadvantage of wood is its hygroscopicity. Moist wood is vulnerable to attack by fungi and termites, making it lose its dimensional stability. The main reason for its hygroscopicity is that the wood fibers present a polar surface associated to the hydroxylated nature of the constituting anhydroglucose units. Such feature is responsible for the high hydrophilicity of wood, enabling the establishment of strong hydrogen bonding between fibers and the formation of three-dimensional wood. On the other hand, the presence of these hydrophilic groups can promote the nucleation and growth of inorganic phases such as TiO_2 and SiO_2 [1–13] on the wood surface, thus producing organic–inorganic hybrid materials. These inorganic particles are usually generated from their monomeric precursors containing reactive organic groups to build up chemical bonds to the hydroxyl groups of wood. Encountering the hydroxyl groups of wood, the monomeric precursors would be hydrolyzed, generating inorganic particles and reactive organic groups with the continuous condensation reactions to form a solid inorganic coating on the wood surface. Our previous research has proven that TiO_2 could be grown on the wood surface with the origin of the hydrophilic groups of the wood [6]. TiO_2 has been extensively studied as a photocatalyst because of its chemical stability and non-toxicity. TiO_2 mainly exists in four polymorphs in nature: anatase (tetragonal, space group $I4_1/amd$), rutile (tetragonal, space group $P4_2/mnm$), brookite (orthorhombic, space group *Pbca*), and TiO_2(B) (monoclinic, space group *C*2/*m*). The anatase phase of TiO_2 has long been considered the most photoactive of these four phases [2, 11, 14–17]. Therefore, TiO_2–wood hybrid materials can enlarge the domination of wood and yield many interesting properties such as hydrophobic and photocatalytic features for removing pollutants.

Inspired by surface topography-induced superhydrophobicity of lotus leaves [18, 19] and water strider's legs [20], a barrier TiO_2 coating could also be grown on wood surface to exhibit hydrophobic properties for meeting higher water repellent requirements of wood or wood-based products. There have been numerous reports regarding the successful

Q. Sun · Y. Lu · Y. Liu (✉)
Key Laboratory of Bio-based Material Science and Technology,
Ministry of Education, Northeast Forestry University,
No. 26 Hexing Road, Harbin, Heilongjiang 150040,
People's Republic of China
e-mail: yxliu@nefu.edu.cn

generation of a hydrophobic surface (water contact angle > 150°) on a substrate surface utilizing laser/plasma etching [21, 22], vertical alignment of nanotube/nanofibers [19, 22, 23], lithographic patterning [16, 24, 25], phase separation [26, 27], binary colloidal assembly [28], glancing angle deposition [29], sol–gel method [10, 30, 31], and so on [32–35]. However, to the best of our knowledge, using the hydrothermal method to grow superhydrophobic TiO_2 on wood surface has not yet been reported. Hydrothermal process is normally conducted in steel pressure vessels called autoclaves with or without Teflon liner under controlled temperature and/or pressure with the reaction in aqueous solutions. The temperature can be elevated above the boiling point of water or other solutions, reaching the pressure of vapor saturation. The temperature and the amount of solution added to the autoclave largely determine the internal pressure produced. Hydrothermal process is a promising method widely used for the production of nanomaterials in many fields, as well as in the fabrication of wood–inorganic hybrid materials. In the present research, hydrophobic and superhydrophobic TiO_2 were grown on the wood surface using hydrothermal method with characterizations of scanning electron microscope (SEM), energy dispersive X-ray spectroscopy (EDS), X-ray diffraction (XRD), and Fourier transform infrared spectroscopy (FTIR), and the measurement of water contact angle (WCA). With the regulation of the reaction conditions, the WCAs could be varied. Thus, controlled hydrophobicity of treated wood could be achieved for the different requirements. The influence of experimental parameters on the hydrophobicity of treated wood was also investigated.

Experimental

Materials

All chemicals were supplied by Shanghai Boyle Chemical Co., Ltd. and used as received. Polar wood slices 20 mm (longitudinal) × 20 mm (tangential) × 10 mm (radial) were ultrasonically rinsed in deionized water for 30 min and dried in vacuum at 80 °C for 24 h.

Synthetic procedure of TiO_2 grown on wood surface

The synthetic conditions used for the growth of TiO_2 on the wood surface are shown in Table 1. A typical TiO_2 growth on the wood surface is described as follows. Tetrabutyl orthotita (TBOT) was first dissolved in anhydrous ethyl alcohol (EtOH) in a 500 ml glass container with magnetic stirring for 30 min and then transferred into a Teflon-lined stainless-steel autoclave. The pending wood samples were then added in the Teflon container for the first hydrothermal process. When finished, 10.2×10^{-4} mol/L sodium dodecyl sulfate (SDS) solution with different pH values were added and reheated at 70 °C for 4 h. Finally, the prepared samples were removed from the solution, ultrasonically rinsed with deionized water for 30 min, and dried at 45 °C for over 24 h in vacuum. For comparative studies, the blank wood samples were also selected.

Table 1 Synthetic condition for growing TiO_2 on wood surface

Samples	Temperature (°C)	pH	TBOT (g)	Time (h)	WCA (°)
S1	70	3	5	4	102
S2	70	6.72	5	4	92
S3	70	9.54	5	4	85
S4	70	3	10	4	101
S5	70	3	40	4	104
S6	70	3	5	8	115
S7	90	3	5	4	123
S8	90	6.72	5	4	96
S9	90	9.54	5	4	91
S10	90	3	5	8	135
S11	110	3	5	4	142
S12	130	3	5	4	154

Characterizations and measurement of WCA

The morphology and elemental compositions of the wood samples were examined by SEM (Quanta 200, FEI) combined with energy dispersive X-ray spectroscopy (EDS, Genesis, EDAX). The crystalline phase of TiO_2 was determined by XRD (D/MAX 2200, Rigaku) with Cu Kα radiation ($\lambda = 1.5418$ Å) at a scan rate (2θ) of 4°/min^{-1}. Accelerating voltage and applied current were 40 kV and 30 mA, respectively, ranging from 5° to 70°. FTIR spectra for the wood samples were recorded using FTIR (Magna-IR 560, Nicolet). A contact angle analyzer (JC2000C) at ambient temperature with a droplet volume of 5 μL was employed to measure the WCA of the samples. An average of five measurements taken at different positions on each sample was applied to calculate the final WCA angle.

Results and discussion

Figure 1 shows the EDS spectra of the blank and treated wood samples. The presence of a significant Ti peak at about 4.6 keV in the spectra of the treated sample suggests that TiO_2 was grown on the wood surface through the hydrothermal process.

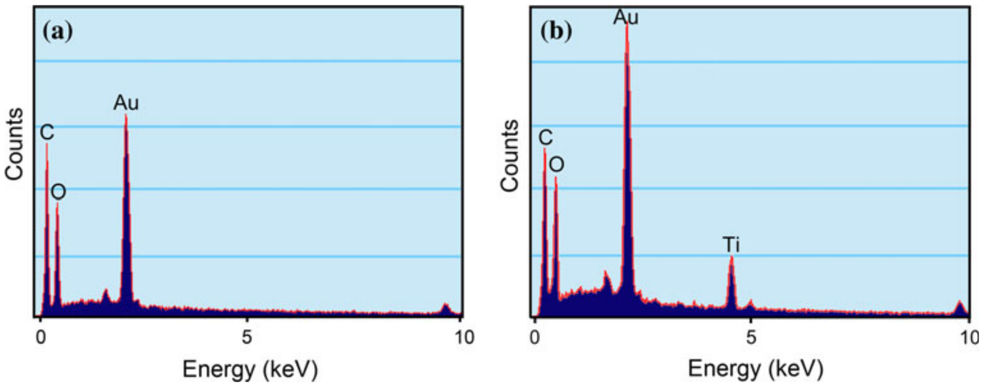

Fig. 1 The EDS spectra of the **a** blank and **b** treated wood

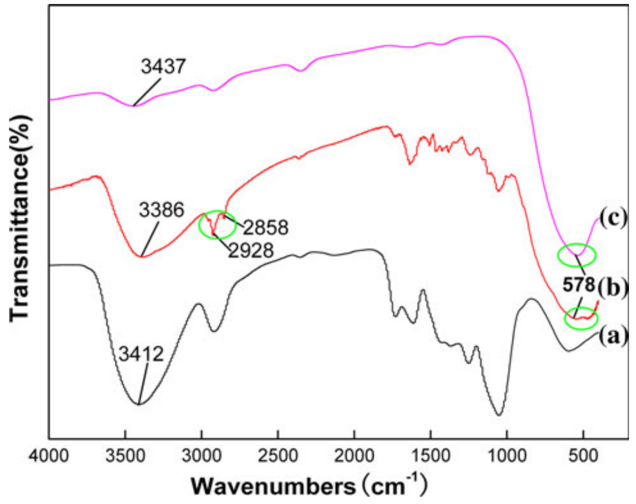

Fig. 2 FT–TR spectra of **a** the treated wood, **b** the control wood, and **c** nano-TiO_2

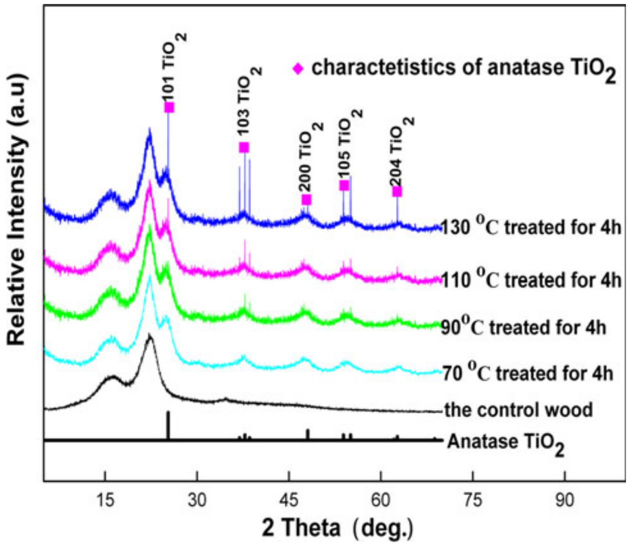

Fig. 3 XRD patterns of the control and treated wood at different temperatures

Figure 2 shows the FTIR spectra of (a) the treated wood, (b) the control wood, and (c) the nano-TiO_2. Similar studies [7, 9, 13, 36–38] were demonstrated that cellulosic fibers or wood could be acted as hydrophilic substrates to the nucleation and growth of inorganic particles, such as SiO_2 and TiO_2. The peaks at 3380–3440 cm^{-1} corresponding to the stretching vibrations of the hydroxyl groups in the treated wood shifted to lower wavenumbers, indicating a strong interaction between the hydroxyl groups of wood surface and the grown TiO_2 nanoparticles through the hydrogen bond. This strong interaction led to the immobilization of TiO_2 nanoparticles in the wood matrix. The peaks at 2928 and 2858 cm^{-1} correspond to $–CH_3$ asymmetric and $–CH_2$ symmetric stretch vibrations [39], respectively. The origin of $–CH_3$ and $–CH_2$ is the SDS incorporated into the TiO_2 surface. These groups provided the hydrophobicity of the treated wood. The peak at 578 cm^{-1} was characteristic of the grown TiO_2 on the wood surface attributed to the Ti–O–Ti stretch vibration. The wide band observed in the frequency range of 800–500 cm^{-1} was the feature of TiO_2 [40]. The formation mechanism of TiO_2 particles is mainly ascribed to the hydrolysis of Ti(IV) and the nature of the Ti(IV) solute precursors as shown in Eqs. 1, 2, and 3 [41].

$$\mathrm{Ti(OC_4H_9)_4 + 4C_2H_5OH \rightarrow Ti(OC_2H_5)_4 + 4C_4H_9OH} \tag{1}$$

$$\mathrm{Ti(OC_2H_5)_4 + 4H_2O \rightarrow Ti(OH)_4 + 4C_2H_5OH} \tag{2}$$

$$\mathrm{mTi(OH)_4 \rightarrow mTiO_2 + 2mH_2O} \tag{3}$$

FTIR spectra further confirmed that TiO_2 was grown on the wood surface and chemically bonded to it through the hydrogen groups during the hydrothermal process.

To characterize the crystal structure of the grown TiO_2, XRD patterns (Fig. 3) of blank and treated wood at different temperatures were measured. The peaks were observed at values of 2θ equal to 25.4°, 37.9°, 48.1°, and 54.5°, which correspond to the anatase structure. XRD patterns also confirmed that anatase TiO_2 was grown on the

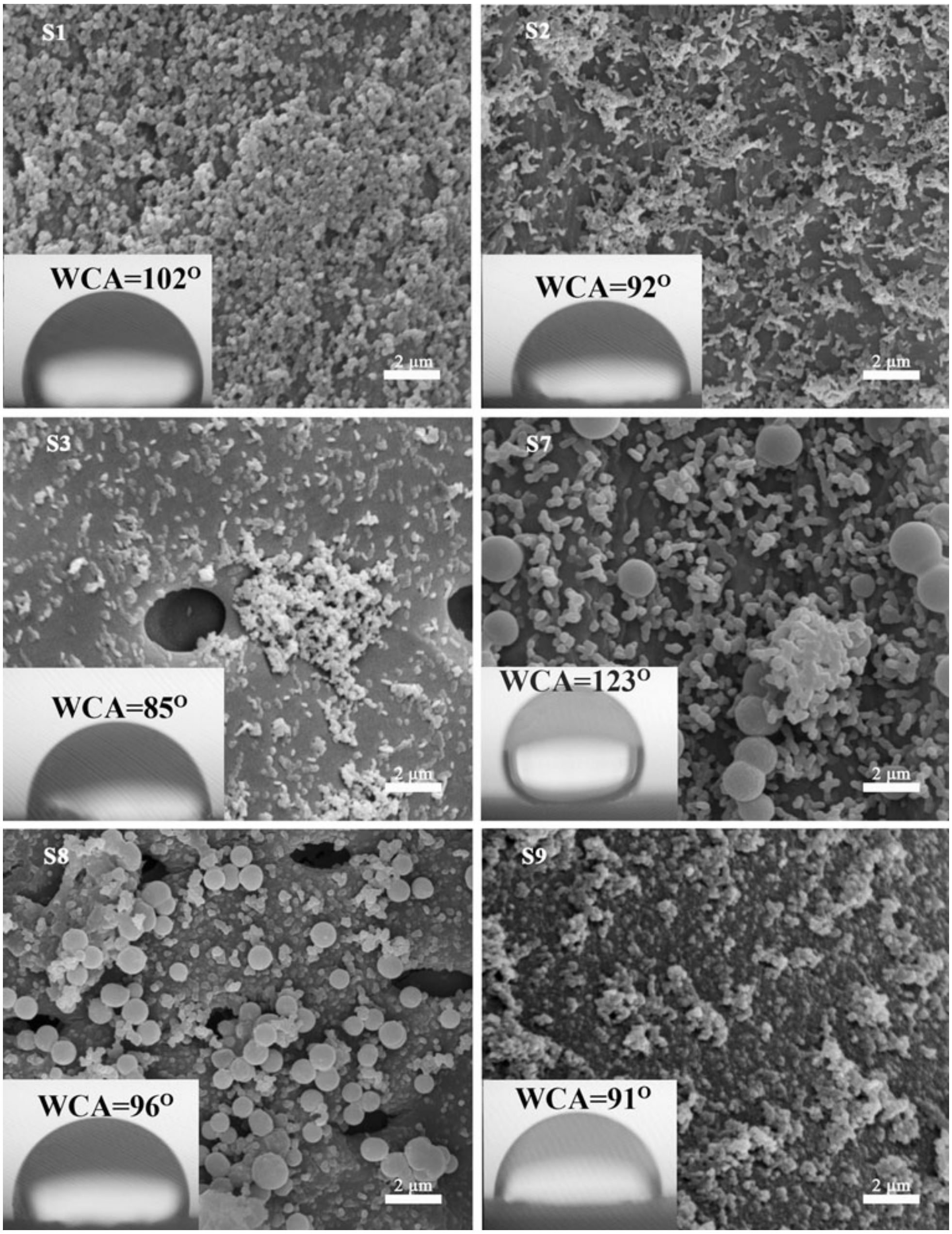

Fig. 4 SEM images of S1, S2, and S3 at 70 °C and S7, S8, and S9 at 90 °C obtained at different pH values, respectively

wood surface via hydrothermal method. The stronger peak intensities of the grown TiO_2 presented in Fig. 3 are attributed to the higher reacting temperatures. Higher temperature leads to a better crystal structure [42]. Therefore, the higher the temperature employed in the experiment, the better the crystalline TiO_2 structure grown on the wood surface.

The above characterizations proved that anatase TiO_2 chemically bonded to the wood surface through the interaction of hydrogen groups during the hydrothermal process. To determine the influence of the experimental parameters on the hydrophobicity of the treated wood, a systemic investigation was carried out according to Table 1.

Table 1 lists the different synthetic conditions adopted to grow TiO_2 on the wood surface. The influence of experimental parameters such as reaction pH, temperature, reaction time, and reactants quality on the hydrophobicity and morphology of the TiO_2-treated wood was characterized from the SEM images and pictures of captured droplet.

The influence of pH values employed by the reaction system on hydrophobicity was investigated at 70 and 90 °C. Results revealed that the lower the pH values used, the larger the WCA retained (Fig. 4). Keeping other variables constant, when the pH value changed from 1 to 10, WCA decreased with the increase of pH value. The WCAs at 70 °C of S1, S2, and S3 with the corresponding pH values were 102°, 92°, and 85°, respectively. Hydrophobicity greatly improved compared with 56° of the control. WCAs at 90 °C of S7, S8, and S9 with different pH values were 123°, 96°, and 91°. WCA decreased with the increase of the pH values. At acidic condition, the treated wood transformed from hydrophilic to hydrophobic. More TiO_2 also grew on the wood surface with a pH of 3 compared to that of 6.72 and 9.54. This indicated that much more $–CH_2$ groups of SDS would attach to the surface of the grown TiO_2 on the wood surface, leading to an increase of WCA. From the analysis, we conclude that the WCA of the treated wood was significantly affected by the reaction's pH. In acid conditions, the hydrophilic wood achieved higher WCA, implying better hydrophobicity for treated wood. Based on Fig. 4, the hydrophobicity of treated wood was enhanced with the increase of reaction temperature. Thus, the influence of reacting temperature on the hydrophobicity of treated wood at a fixed pH value of 3 should be investigated.

Temperature has a significant influence on the hydrophobicity and morphology of grown TiO_2. Keeping other variables constant, when the reaction temperature changed from 70 to 90, 110, and 130 °C, the relevant WCAs of the treated wood were 102°, 123°, 142°, and 154° of S1, S7, S11, and S12, respectively (Figs. 4, 5). The morphologies emerged as particles: sphere accompanying rod-like TiO_2, complete sphere TiO_2, and complete rod-like TiO_2. The increase of WCAs could be attributed to the enlargement of the $–CH_2$ groups belonging to SDS, as already proven by the FTIR spectra (Fig. 2). The hydrolysis extension of the Ti(IV) precursor favors enhanced temperatures. The higher the temperature employed, the more TiO_2 grown are on the wood surface. This results in considerably more $–CH_2$ groups bonding to grown TiO_2. Therefore, hydrophobicity of the treated wood increased with enhanced reaction temperature under a fixed pH value of 3. Superhydrophobic wood treated at 130 °C was achieved. From the supporting information, the water droplet could smoothly roll from the treated wood surface.

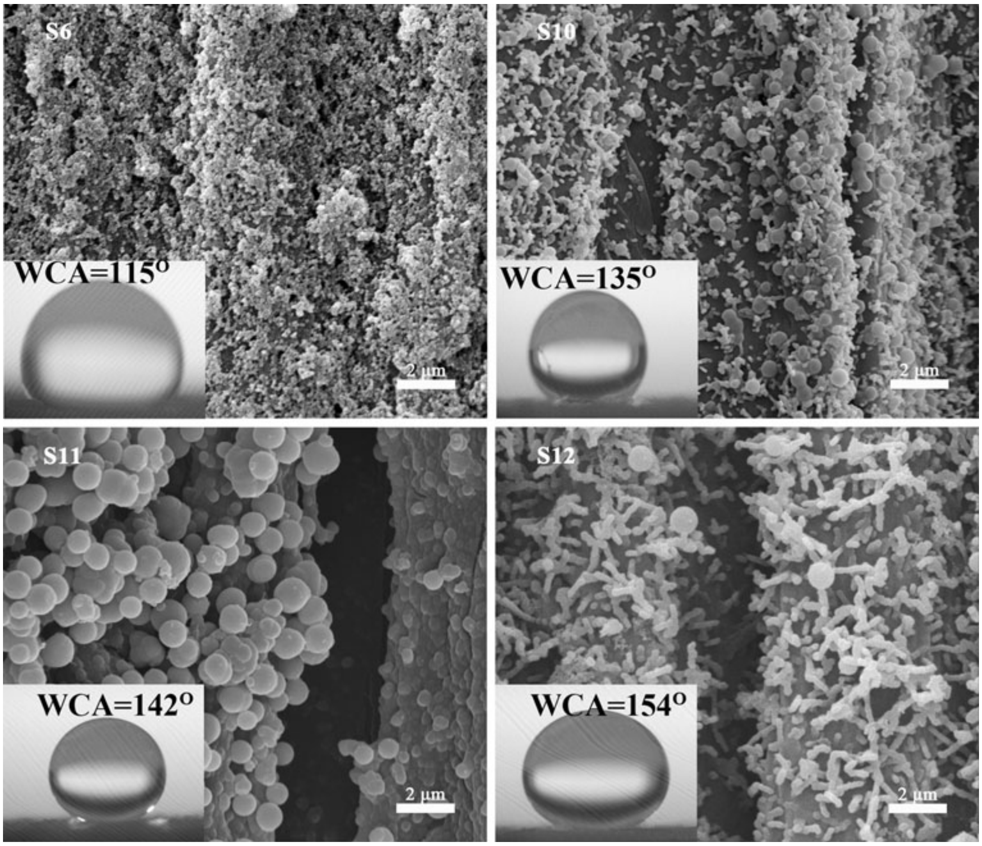

Fig. 5 SEM images of S11 and S12 obtained at 110 and 130 °C, respectively with the fixed pH value of 3

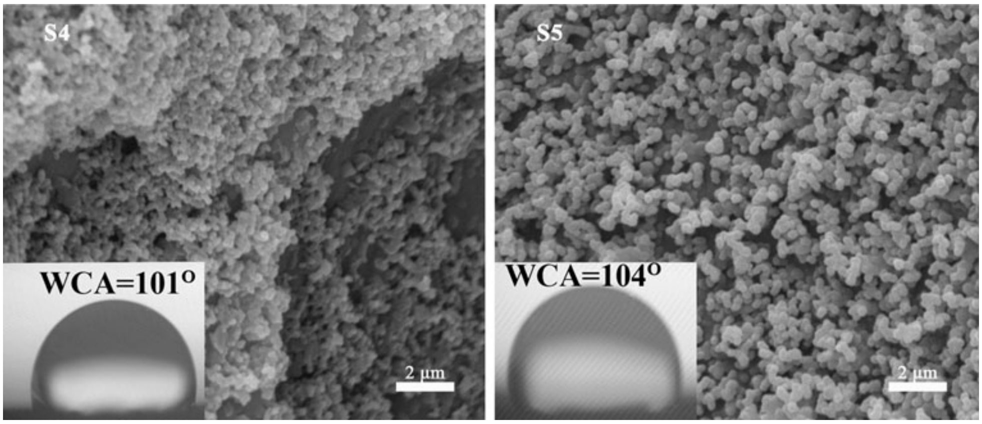

Fig. 6 SEM images of S4 with 10 g and S5 with 40 g of the amount of TBOT

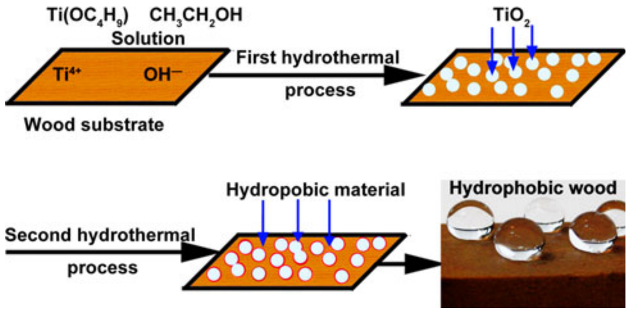

Fig. 7 Schematic illustrations for fabricating the hydrophobic wood using the hydrothermal method

Keeping other variables constant, the extension of reaction time also led to bigger WCAs (Fig. 6). When reaction times of 4 and 8 h were employed, comparing S1 and S6 and S7 and S10, the WCAs of the treated samples increased from 102° to 115° and 123° to 135°, respectively. The relevant SEM images are exhibited in Figs. 4 and 6. The grown TiO_2 nanoparticles were densely dispersed on the wood surface with the extended reaction time. The hydrophobicity was mainly due to the increment of the $–CH_2$ groups bonding to the grown TiO_2. With the 5–40 g amount of the TBOT precursor in the starting solution, there was an obvious effect on the amount of grown TiO_2 (Fig. 6). The WCAs of S4 and S5 only had slight increases, which changed from 101° to 104°.

From the above investigation of the experimental parameters for hydrophobic TiO_2 grown on the wood surface, its possible mechanism could be described as follows. In hydrothermal conditions, the grown TiO_2 underwent the following processes: (1) TBOT in EtOH solution alcoholized to generate Ti^{4+} and many hydrophilic –OH groups, (2) Ti^{4+} in the mixed solution and $\mathrm{O\bar{H}}$ reacted to generate $Ti(OH)_{4,}$ (3) $Ti(OH)_4$ continued alcoholysis to generate a certain structure of TiO_2 nuclei with the help of hydrothermal energy, (4) With the introduction of the hydrophobic chemical groups, the treated wood achieved hydrophobic property to prevent the invasion of water droplet under the second hydrothermal process. Hydrothermal reaction schematic illustrations are shown in Fig. 7.

Conclusions

Hydrophobic anatase TiO_2 chemically bonded to the wood surface through hydrogen groups using a hydrothermal method was achieved. During the hydrothermal process, the hydrophilic wood was converted to hydrophobic or superhydrophobic wood. Through systemic investigation of experimental parameters, pH value and temperature were found to have a significant influence on the hydrophobicity of treated wood. The lower the pH value and the higher the temperature employed, the larger the WCA achieved. The temperature had a remarkable effect on the morphologies of the grown TiO_2 of the treated wood. The hydrophobic mechanism of the treated wood was mainly attributed to the introduction of CH_2 groups belonging to SDS. This study also provided a feasible method to fabricate wood (fiber, bamboo, and paper)/inorganic hybrid materials.

Acknowledgement This study was financially supported by the Breeding Plan of Excellent Doctoral Dissertation of Northeast Forestry University (GRAP09) and the Programme of Introducing Talents of Discipline to Universities of China (B08016).

References

1. Barata MAB, Neves MC, Pascoal Neto C, Trindade T (2005) Dyes Pigments 65:125
2. Hübert T, Unger B, Bücker M (2010) J Sol Gel Sci Technol 53:384
3. Kim GG, Kang JA, Kim JH, Kim SJ, Lee NH, Kim SJ (2006) Surf Coat Technol 201:3761

4. Kim TK, Lee MN, Lee SH, Park YC, Jung CK, Boo JH (2005) Thin Solid Films 475:171
5. Kuroda A, Joly P, Shibata N, Takeshige H, Asakura K (2008) J Am Oil Chem Soc 85:549
6. Li J, Yu H, Sun Q, Liu Y, Cui Y, Lu Y (2010) Appl Surf Sci 256:5046
7. Marques PAAP, Trindade T, Neto CP (2006) Compos Sci Technol 66:1038
8. Miyafuji H, Saka S (1997) Wood Sci Technol 31:449
9. Schmalzl KJ, Evans PD (2003) Polym Degrad Stab 82:409
10. Tadanaga K, Morinaga J, Matsuda A, Minami T (2000) Chem Mater 12:590
11. Yang D, Xu Y, Wu D, Sun Y, Zhu H, Deng F (2006) J Phys Chem C 111:999
12. Tshabalala M, Gangstad J (2003) J Coat Technol 75:37
13. Tshabalala M, Sung L (2007) J Coat Technol 4:483
14. Yang D, Liu H, Zheng Z, Yuan Y, Zhao J, Waclawik ER, Ke X, Zhu H (2009) J Am Chem Soc 131:17885
15. Yang D, Zheng Z, Zhu H, Liu H, Gao X (2008) Adv Mater 20:2777
16. Yang H, Deng Y (2008) J Colloid Interface Sci 325:588
17. Kibanova D, Trejo M, Destaillats H, Cervini-Silva J (2009) Appl Clay Sci 42:563
18. Feng L, Li S, Li Y, Li H, Zhang L, Zhai J, Song Y, Liu B, Jiang L, Zhu D (2002) Adv Mater 14:1857
19. Feng X, Zhai J, Jiang L (2005) Angew Chem Int Ed 44:5115
20. Gao X, Jiang L (2004) Nature 432:36
21. Baldacchini T, Carey JE, Zhou M, Mazur E (2006) Langmuir 22:4917
22. Jin M, Feng X, Feng L, Sun T, Zhai J, Li T, Jiang L (2005) Adv Mater 17:1977
23. Feng L, Li S, Li H, Zhai J, Song Y, Jiang L, Zhu D (2002) Angew Chem Int Ed 41:1221
24. Fürstner R, Barthlott W, Neinhuis C, Walzel P (2005) Langmuir 21:956
25. Öner D, McCarthy TJ (2000) Langmuir 16:7777
26. Nakajima A, Abe K, Hashimoto K, Watanabe T (2000) Thin Solid Films 376:140
27. Zhao N, Xu J, Xie Q, Weng L, Guo X, Zhang X, Shi L (2005) Macromol Rapid Commun 26:1075
28. Zhang G, Wang D, Gu Z, Möhwald H (2005) Langmuir 21:9143
29. Tsoi S, Fok E, Sit JC, Veinot JGC (2004) Langmuir 20:10771
30. Erbil HY, Demirel AL, Avcı Y, Mert O (2003) Science 299:1377
31. Shirtcliffe NJ, Mchale G, Newton MI, Perry CC, Roach P (2005) Chem Commun 25:3135
32. Guo Z, Zhou F, Hao J, Liu W (2005) J Am Chem Soc 127:15670
33. Ming W, Wu D, van Benthem R, de With G (2005) Nano Lett 5:2298
34. Sun M, Luo C, Xu L, Ji H, Ouyang Q, Yu D, Chen Y (2005) Langmuir 21:8978
35. Tavana H, Amirfazli A, Neumann AW (2006) Langmuir 22:5556
36. Amberg-Schwab S, Hoffmann M, Bader H, Gessler M (1998) J Sol Gel Sci Technol 13:141
37. Saka S, Ueno T (1997) Wood Sci Technol 31:457
38. Mahltig B, Swaboda C, Roessler A, Böttcher H (2008) J Mater Chem 18:3180
39. Pandey KK (1999) J Appl Polym Sci 71:1969
40. Colomer MT, Velasco MJ (2007) J Eur Ceram Soc 27:2369
41. Wu R, Wei Y, Zhang Y (1999) Mater Res Bull 34:2131
42. Zhang J, Xiao X, Nan J (2010) J Hazard Mater 176:617